Phase coexistence in a DLVO model of globular protein solutions

2003 J. Phys.: Condens. Matter 15 375

(http://iopscience.iop.org/0953-8984/15/3/305)

INSTITUTE OF PHYSICS PUBLISHING JOURNAL OF PHYSICS: CONDENSED MATTER

J. Phys.: Condens. Matter **15** (2003) 375–384 PII: S0953-8984(03)52764-3

Phase coexistence in a DLVO model of globular protein solutions

G Pellicane[1], **D Costa and C Caccamo**

Istituto Nazionale per la Fisica della Materia (INFM), Italy
and
Dipartimento di Fisica, Università di Messina, Contrada Papardo, CP 50, 98166 Messina, Italy

E-mail: pellican@tritone.unime.it

Received 7 August 2002
Published 13 January 2003
Online at stacks.iop.org/JPhysCM/15/375

Abstract

Globular protein solutions of lysozyme in water and added salt are modelled according to the Derjaguin–Landau–Verwey–Overbeek (DLVO) theory, in order to determine their fluid–fluid and fluid–solid coexistence lines. Calculations are based on both computer simulations and theoretical approaches. Our results indicate that, when the potential parameters are obtained by fitting physical properties directly deducible from either static or dynamic light scattering data, the fluid–fluid phase coexistence predictions agree quite well with the experiments. Our description of the solid phase allows only a qualitative reproduction of the experimental solubility boundaries. The overall accuracy of our predictions is discussed in view of the well known limitations of the DLVO representation of protein solutions.

Current interest in simple models of protein solutions is mainly related to the possibility of successfully predicting the most favourable conditions for protein crystallization [1], a process whose control is of crucial importance for the determination of protein structure. Experimental results actually suggest that the best conditions for crystal growth from the solutions are met when the fluid–fluid coexistence—which for such systems consists in the equilibrium between a protein-rich and a protein-poor phase—becomes metastable with respect to the solid–fluid equilibrium, the critical point falling just beneath the solubility line [2–4]. A number of experimental observations also show that protein crystallization usually occurs in a narrow interval of small negative values of the second virial coefficient B_2 [5], termed the 'crystallization slot'. This evidence, interpreted in terms of an effective short-range pair interaction between the macromolecules [3], and the further assumption of uniformly charged

[1] Author to whom any correspondence should be addressed.

0953-8984/03/030375+10$30.00

protein surfaces, have prompted several authors to the application of the Derjaguin–Landau–Verwey–Overbeek (DLVO, [6]) and other theories of colloids to protein solutions [7–10].

The metastability of the fluid–fluid with respect to the fluid–solid coexistence characterizes the phase diagram of a wide class of short-range pair potentials [11], for instance the hard-core Yukawa [12], the adhesive hard-sphere [3, 4, 13] and the $2n - n$ Lennard-Jones type potentials [14], or the α-Lennard-Jones potential used in the description of protein–protein interactions in [2].

The DLVO potential belongs to the same class of force laws, given a sufficiently high ionic strength of the solution (typically greater than 0.2 M). We recall that the analytical form of the DLVO potential is written as the sum of a short-range attractive van der Waals term,

$$v_{\mathrm{HA}}(r) = -\frac{A_{\mathrm{H}}}{12}\left[\frac{\sigma^2}{r^2} + \frac{\sigma^2}{r^2-\sigma^2} + 2\ln\frac{r^2-\sigma^2}{r^2}\right], \tag{1}$$

and a Coulomb, Debye–Hückel-like contribution,

$$v_{\mathrm{DH}}(r) = \frac{1}{4\pi\epsilon_0\epsilon_{\mathrm{r}}}\left[\frac{z_{\mathrm{p}}e}{1+\chi_{\mathrm{DH}}\sigma/2}\right]^2 \frac{\exp[-\chi_{\mathrm{DH}}(r-\sigma)]}{r}. \tag{2}$$

Here σ is the hard-sphere diameter, A_{H} is the Hamaker constant, $Q = z_{\mathrm{p}}e$ is the net charge on the particle in electron units, ϵ_{r} and ϵ_0 are the (solution) relative and the vacuum dielectric constants, respectively, and χ_{DH} is the inverse Debye screening length, related to the solution ionic strength I_{s} by the following expression [15]:

$$\chi_{\mathrm{DH}} = [4\pi L_{\mathrm{b}} 1000 N_{\mathrm{A}} I_{\mathrm{s}}]^{1/2}, \tag{3}$$

where $L_{\mathrm{b}} = e^2/(2\pi\epsilon_0\epsilon_{\mathrm{r}}k_{\mathrm{B}}T)$ is the Bjerrum length, k_{B} is the Boltzmann constant and N_{A} is the Avogadro number. A cut-off value δ, typically envisioned as the thickness of the Stern layer, is introduced in order to circumvent the singularity of the van der Waals contribution to the potential (1) [9, 16]. With these notations, the DLVO potential is written as

$$v_{\mathrm{DLVO}}(r) = \begin{cases} \infty & r < \sigma + \delta \\ v_{\mathrm{HA}}(r) + v_{\mathrm{DH}}(r) & r \geqslant \sigma + \delta. \end{cases} \tag{4}$$

In the low-ionic-strength regime, the electrostatic repulsive contribution prevails over the attractive term beyond a certain distance, in such a way that $v_{\mathrm{DLVO}}(r)$ exhibits, after an initial negative region, a positive bump asymptotically decaying to zero (the well known DLVO potential barrier). In figure 1 we show instead the different shape that $v_{\mathrm{DLVO}}(r)$ assumes for several specific sets of potential parameters, suited to describe solutions characterized by a relatively high ionic strength. These parameters (reported in table 1 along with the corresponding salt molarities to be investigated in this work) have been determined by Muschol and Rosenberger [9] and Beretta and co-workers [17], in order to rationalize static and dynamic light scattering experiments on lysozyme in water–NaCl or water–$(NH_4)_2SO_4$ solutions. These authors calculated, in particular, the slope of the scattered intensity data k_{S} and of the collective diffusion coefficient k_{D}, as a function of the solution ionic strength I_{s}, and on such a basis described the protein interaction through a DLVO representation. The experimental data and the theoretical curves obtained in [9] and [17] are reproduced in figure 2; it appears that different molar ranges have been encompassed in the two experiments, and that the DLVO performances are semiquantitative in the low-molarity NaCl-added solution and qualitative for the high-ionic-strength $(NH_4)_2SO_4$-added solutions. It is worth observing that the Hamaker constant, the protein charge and the Stern layer thickness, that have been used as adjustable parameters, do actually fall in a range commonly accepted on the basis of much experimental evidence [9, 17].

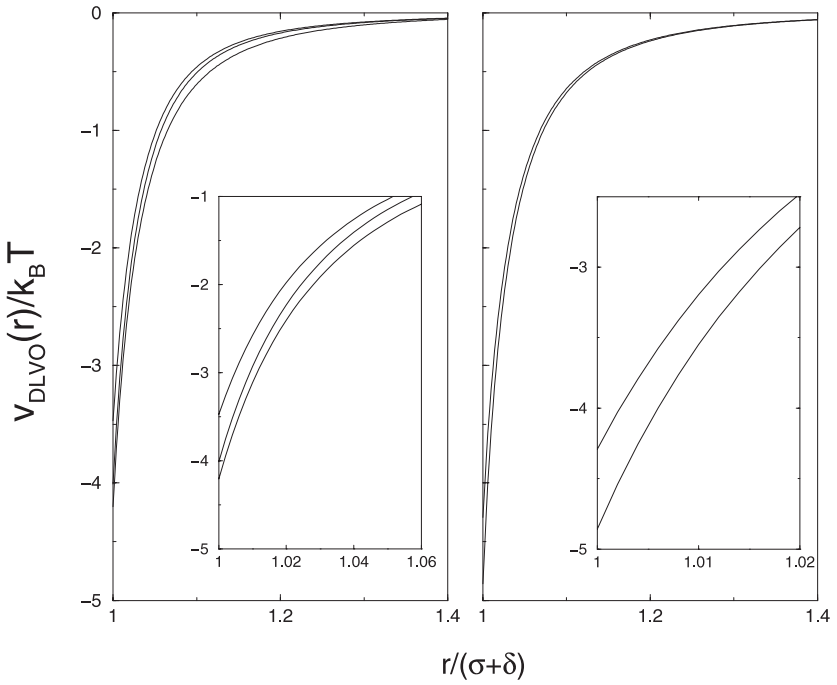

Figure 1. Left: DLVO models A, B1 and B2 of table 1 (from top to bottom). Right: potential patterns for sets B3 and C (from top to bottom). Insets show a magnification of the region immediately outside the hard core. The energy and length units are reported in table 1.

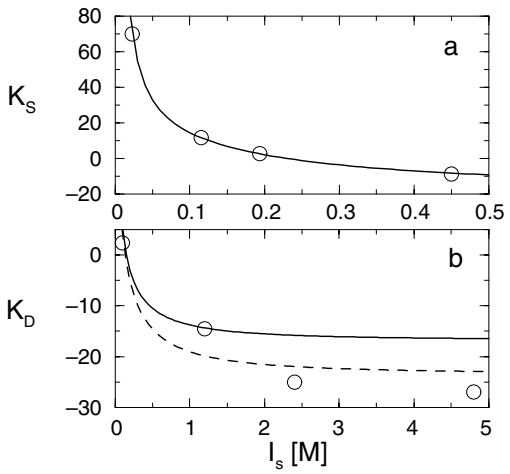

Figure 2. Top: slope of the scattered intensity data k_S versus the ionic strength in water + NaCl solutions of lysozyme. Circles, experimental points; curve, overall DLVO best fit (set A in table 1) [9]. Bottom: slope of the collective diffusion coefficient, k_D, in water + $(NH_4)_2SO_4$ lysozyme. Circles, experimental points; full curve, DLVO fit of k_D at $I_s = 1.2$ M (sets B); dashed curve, overall DLVO best fit (set C) [17].

In order to assess the performances of a DLVO approach in predicting the fluid–fluid and fluid–solid equilibria in real globular protein solutions, we shall compare in the following

Table 1. Parameters of the DLVO model of equation (4) investigated in this work. The Hamaker constant A_H is given in k_BT units at $T = 293$ K, the protein charge Q in electron units and the thickness of the Stern layer δ in nm; the protein diameter is $\sigma = 3.6$ nm. A_H, Q and δ for set A are taken from [9], those for sets B and C from [17]. The three salt molarities I_s in the last column correspond to the experimental conditions investigated in [10].

Model	A_H	Q	δ	I_s
A	8.1	10.7	0.180	0.51
B1	8.0	10.0	0.164	0.51
B2	8.0	10.0	0.164	0.85
B3	8.0	10.0	0.164	1.20
C	8.0	10.0	0.150	1.20

theoretical and simulation results based on the parameters of table 1, with the experimental phase diagrams for solutions of lysozyme in water and NaCl at 0.51, 0.85 and 1.2 M ionic strength, determined in another work of Muschol and Rosenberger [10]. These authors investigated in detail, through light scattering intensity measurements, the demixing conditions of the solution in protein-rich and a protein-poor phases and, by comparing with the solubility lines calculated by others [18, 19], found that the fluid–fluid separation is always metastable with respect to the fluid–solid coexistence. The parameters of the DLVO model reported in table 1 have been associated with the different molarities according to the following procedure.

- *Model A.* For the 0.51 M fluid–fluid phase separation, we retain the values of A_H, Q and δ used in [9] to best fit the experimental k_S versus I_s up to 0.427 M of added NaCl (see the top panel of figure 2). We are in fact not aware of other k_S determinations for higher NaCl molarities.
- *Models B.* Forced by the lack of experimental data for the high-NaCl-molarity solutions, and in the spirit of an ample investigation of the phase diagram for the three regimes envisaged in [10], we resort to the $[A_H, Q, \delta]$ set determined in [17] to fit k_D at 1.2 M in $(NH_4)_2SO_4$-added solution (see figure 2, bottom panel).
- *Model C.* The $[A_H, Q, \delta]$ set that corresponds to the overall best fit of k_D versus I_s shown in the bottom panel of figure 2 [17] has been used to calculate the fluid–fluid coexistence for the 1.2 M NaCl solution.

We always fix the protein diameter $\sigma = 3.6$ nm.

Phase equilibria for models A–C of table 1 have been determined according to different methods. In particular, the fluid–fluid phase boundaries have been studied through a Gibbs ensemble Monte Carlo (GEMC, [20]) approach. We have performed 100 000 standard GEMC steps at each temperature considered, on samples composed of $N = 512$–1024 particles, in order to equilibrate the system, followed by five to ten cumulation runs of the same length. Depending on the temperature, 1000–7000 trials to swap particles between the two boxes have been attempted.

As far as the solid–fluid equilibrium is concerned, the free energy of the fluid phase has been calculated in the framework of the hybrid mean-spherical approximation [21, 22], by integrating the equation of state from zero up to high densities along isothermal paths. On the solid side, we have determined the free energy through a standard first-order perturbation theory [23], based on a reference solid of hard spheres, whose equation of state and structural functions are known from previous studies [24].

Results for the phase diagrams are shown in figures 3–5. We observe that the critical density and temperature of the fluid–fluid equilibrium are fairly well predicted for all the ionic strengths investigated, with discrepancies from the experimental values that never exceed a

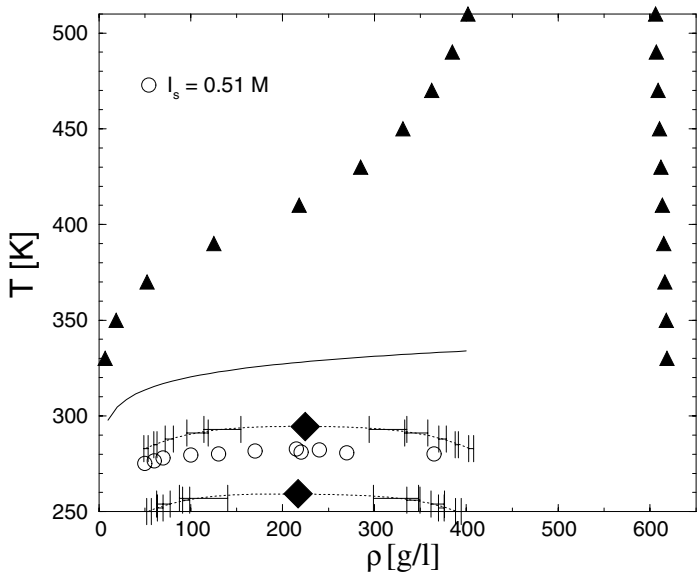

Figure 3. Phase diagram of a lysozyme in water–NaCl solution at $I_s = 0.51$ M. Circles, experimental fluid–fluid coexistence [10]; full curve, experimental solubility boundary of the tetragonal solid phase [10, 18, 19]. Dotted curves with error bars, GEMC fluid–fluid equilibria for the DLVO model A (lower line) and B1 (upper line) of table 1; full diamonds indicate the critical points. Triangles, theoretical free energy determination of the solid–fluid coexistence for model B1.

few per cent. Significantly, the two sets of DLVO parameters employed at 0.51 M, i.e. A and B1 of table 1, lead to phase diagrams which bracket the experimental curve; it thus appears that a more accurate, or even quantitative, reproduction of the experimental curve might be achievable, should an assessed strategy for fixing A_H, Q and δ be devised. The sensitivity of the phase diagram to a fine tuning of the parameters is also evident at 1.2 M, as shown in figure 5, where the difference between the exact (set B3) and the approximate (set C) fit to the experimental k_D (see figure 2(b)) evidently emerges. The effect of varying the Stern layer thickness appears in this context particularly appreciable as already observed in [17]. We recall that this quantity can be related to the intrinsic size of counterions, which condense on the macromolecule surface, and can reasonably attain values of the order of 0.2 nm.

All the 'liquid–vapour' coexistence lines appear metastable with respect to the theoretically determined solid–fluid phase boundaries, in agreement with the experimental evidence. The connection between the second virial coefficient as an indicator for protein crystallization [5], and the presence of a metastable fluid–fluid separation in protein solution, led several authors to investigate the relation between the critical temperature T_c and B_2 (see e.g. [25, 26] and references cited therein). Vliegenthart and Lekkerkerker [25] pointed out, in particular, that the second virial coefficient for several simple model fluids attains a fairly constant value around the critical temperature, namely $B_2^* \equiv B_2(T_c)/v_0 \simeq -6$, where v_0 is the volume of the particle. A similar analysis for the DLVO models envisaged in this study is reported in figure 6, where the behaviour of B_2 as a function of the temperature is shown. An average value with a small dispersion, $B_2^* \simeq (-5.02 \pm 0.06)$ occurs for such systems, in fair agreement with the range $B_2^* = [-5.45 \text{ to } -8.85]$ determined in [25]. We observe that the value $B_2^* \simeq -5.1$, obtained for set A (see figure 6), that best fits the lysozyme in water–NaCl solution at 0.51 M [9], closely corresponds to the experimental outcome $B_2 = -5.3\ v_0 \equiv -2.8 \times 10^{-4}$ mol cm^3 g^{-2}

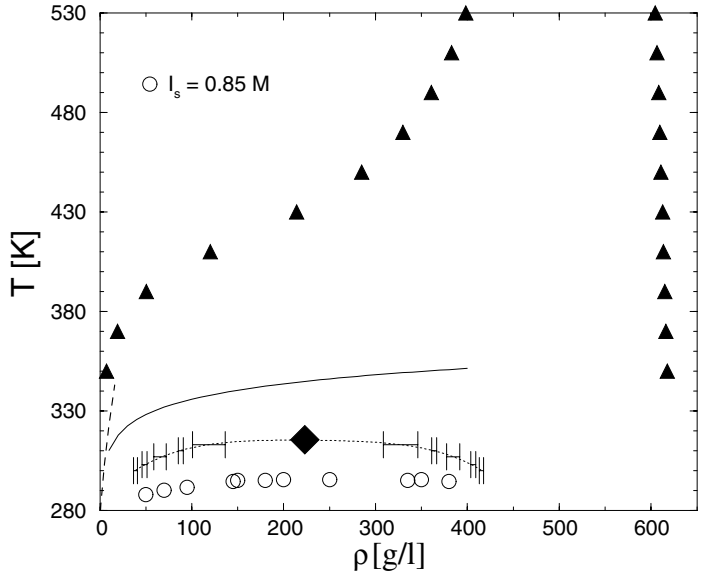

Figure 4. Phase diagram for a lysozyme in water–NaCl solution at $I_s = 0.85$ M. Circles, experimental fluid–fluid coexistence [10]; full and dashed curves, experimental solubility boundary for the tetragonal and orthorhombic solid phases, respectively [10, 19]. Dotted curve with error bars, GEMC fluid–fluid coexistence for DLVO model B2 of table 1; the full diamond indicates the critical point. Triangles, solid–fluid coexistence for model B2.

obtained in [5] for the same solution, around the crystallization slot, at the slightly lower 0.34 M ionic strength. Moreover, models B1–B3 tend to overestimate the critical temperature of the real solutions, as visible in figures 3–5; interestingly, however, the application of the criterion $B_2^* \simeq -6$ would produce in these cases critical temperatures fairly close to the experimental ones (see figure 5).

No experimental data for the solid branch line at high density, to compare our predictions to, are currently available. As far as the fluid branch is concerned, the experimental solubility lines correspond to coexisting solid phases with either tetragonal or orthorhombic symmetry [18, 19], whilst our perturbation approach for the solid phase is based on a inherent FCC hard-sphere structure. This can explain the apparent discrepancy between our predictions and the experimental results, especially as far as the tetragonal line is concerned (see figures 3–5). We observe however that, at variance with the FCC lattice, where each particle is in close contact with 12 neighbours, in a tetragonal lysozyme crystal each protein has strong interactions with four neighbouring molecules [27]; the orthorhombic structure is also characterized by a number of contacts smaller than that of a compact FCC arrangement. Since the potential energy per particle in the crystalline phase at low temperature is given by the value of the pair potential at minimum separation times half the number of nearest neighbours, we expect, in passing from an FCC to a tetragonal or orthorhombic structure, a substantial decrease of the absolute value of the internal energy. Although we cannot predict the quantitative relevance of such a reduction, the general trend of the fluid–solid equilibrium can be surmised from a theoretical investigation carried out in [28], where it is shown that even a tiny decrease of the number of contacts per particle drastically lowers and flattens the sublimation line in a square-well fluid. The same conclusion has been obtained in the simulation study of [12] on a Yukawa model with variable attractive range. On such a basis we can confidently forecast a contraction of the

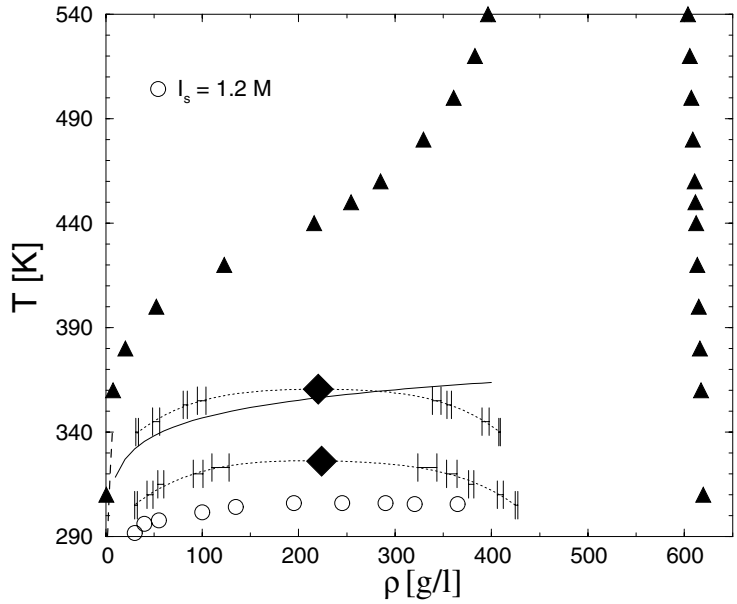

Figure 5. Phase diagram for a lysozyme in water–NaCl solution at $I_s = 1.2$ M. Circles, experimental fluid–fluid coexistence [10]; full and dashed curves, experimental solubility boundary for the tetragonal and orthorhombic solid phase, respectively [10, 19]. Dotted curves with error bars, GEMC fluid–fluid equilibria for DLVO model B3 (lower curve) and C (upper curve) of table 1; diamonds, critical points. Triangles, solid–fluid coexistence for model B3.

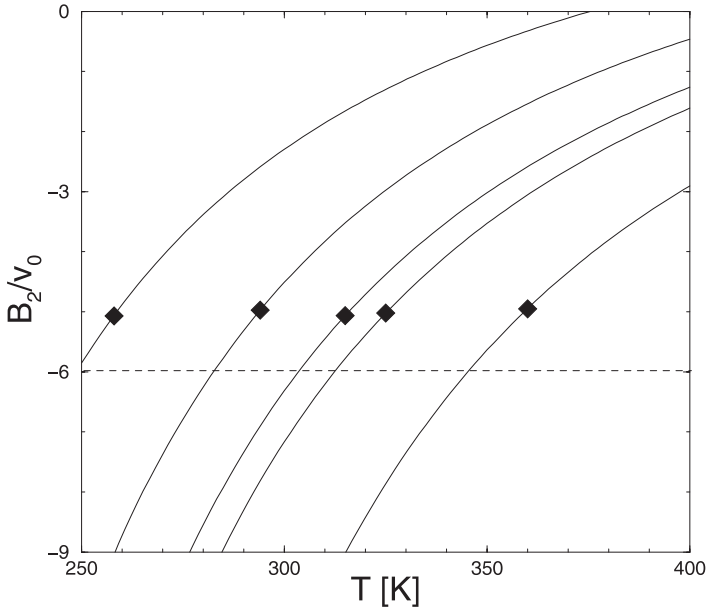

Figure 6. Behaviour of the second virial cofficient B_2 as a function of the temperature for models A, B1, B2, B3 and C of table 1 (from top to bottom). The markers indicate the critical values of each model. The value $B_2/v_0 = -6$ deduced in [25] is also shown (dashed line).

temperature gap between the solubility line and the critical temperature, and hence a closer agreement with the experimental findings, should the correct crystal symmetry be taken into account in our analysis.

As far as a general discussion of the models here employed in order to investigate real globular protein solutions is concerned, we recall that we have used in a number of cases parameters appropriate to fit k_D in ammonium sulfate solutions, whilst comparing with experimental phase diagrams for NaCl solutions [10]. More generally, other serious limitations are intrinsic to a one-component fluid representation, since this latter cannot take into account the large variability of solution conditions such as related, for instance, to cation and anion identity, salt concentration, salt bridges, hydrogen bonding, hydrophobic effects etc [8–10, 15, 29, 30]. Also, a spherically symmetric representation of the interactions cannot describe the surface topology (whose influence seems relevant for the occurrence of a metastable liquid–liquid immiscibility region [27]), as well as the microscopic mechanisms underlying molecular recognition phenomena [31]. The applicability of the DLVO model in the context of biological systems, in particular, has been recently questioned [32, 33].

Some insight into the overall limitations involved in a monodisperse, short-range description of real protein solutions can be gained from several recent investigations that account for the shape anisotropy of the protein [31, 34], or include several 'sticky' sites at the surface of the protein [35, 36]. In particular, the behaviour of the second virial coefficient B_2 in a model where the discrete nature of the solvent and of the charge distribution on the molecular surface are explicitly taken into account has been considered in [36]. It is shown that, for such a model, B_2 has a non-monotonic dependence on the added salt concentration, in agreement with various experimental findings on protein solutions (see [36] and references quoted therein). This feature in the B_2 trend disappears if a smeared charge distribution on the molecular surface is assumed; the DLVO model, based on a spherically symmetric representation of interactions, is similarly unable to reproduce a non-monotonic B_2 behaviour.

A second investigation [37] concerns the kinetics of crystallization of the α-Lennard-Jones fluid, a model introduced to investigate the phase behaviour of protein solutions [2], that is characterized (as is the DLVO potential) by a short-range attractive interaction. In this model the early germination of the solid phase takes place when the system approaches and eventually crosses the metastable binodal line, a result in positive agreement with the experimental observations of [9]. However, the elapsed time for the onset of crystallization is still orders of magnitude lower than that observed in a typical protein solution (hours or days); this result is in qualitative agreement with the observation that the rate of crystallization of moderate ionic strength protein solutions modelled through the DLVO potential is unrealistically high [29].

Despite the intrinsic limitations mentioned above, the success of the DLVO model in reproducing the phase diagram of real protein solutions seems of valuable interest. We argue that the basic mechanisms governing the phase equilibrium in such systems are reasonably well captured by the DLVO representation, in agreement with previous studies on the overall shape of the phase diagram in short-range potential fluids [2–4, 11–13, 32]. Moreover, our investigation shows that the accuracy of the DLVO applications can be brought to even higher standards, provided that the potential parameters are properly chosen. It seems, for this purpose, that the fit of k_S or k_D versus ionic strength data is a good strategy, that however certainly calls for further optimization. To this end more extensive results from light scattering experiments, in solutions with various added salts and over wide molarity ranges, would be valuable.

Extensions of this study, in order to assess the theoretical determination of the solubility lines on the basis of 'exact' computer simulations, are in progress. More extensive investigations of the kinetics of crystallization at higher densities than those envisaged in [37] would also be desirable. It has been recently shown, in fact, that in two different short-range

potential systems one can identify a glass (or possibly gelation) line at relatively high density, falling inside the solid–fluid equilibrium boundaries [38]. The kinetics of cluster aggregation is in general altered in the neighbourhood of such a line; should this latter effectively exist for the α-Lennard-Jones potential, and also for the DLVO model, one could reasonably expect a substantial reduction of the crystallization rate.

Acknowledgments

The authors acknowledge a useful discussion with Professor R Piazza. GP wishes to thank Professor G Chirico for his hospitality and helpful discussions during a visit to the Bio-Spectroscopy Laboratory of the University of Milan.

References

[1] McPherson A 1982 *Preparation and Analysis of Protein Crystals* (Malabar, FL: Krieger)
[2] ten Wolde P R and Frenkel D 1997 *Science* **277** 1975
[3] Rosenbaum D F, Zamora P C and Zukoski C F 1996 *Phys. Rev. Lett.* **76** 150
Rosenbaum D F, Kulkarni A, Ramakrishnan S and Zukoski C F 1999 *J. Chem. Phys.* **111** 9882
[4] Poon W C K 1997 *Phys. Rev.* E **55** 3762
[5] George A and Wilson W 1994 *Acta Crystallogr.* D **50** 361
[6] Derjaguin B V and Landau L V 1941 *Acta Physicochim. USSR* **14** 633
Verwey E J W and Overbeek J T G 1948 *Theory of Stability of Lyophobic Colloids* (Amsterdam: Elsevier)
[7] Chen S-H, Huang J S and Tartaglia P (ed) 1992 *Structure and Dynamics of Strongly Interacting Colloids and Supramolecular Aggregates in Solution* (Dordrecht: Kluwer)
[8] Grant M L and Saville D A 1994 *J. Phys. Chem.* **98** 10358
Kuehner D E, Heyer C, Rämsch C, Fornefeld U M, Blanch H W and Prausnitz J M 1997 *Biophys. J.* **73** 3211
Kulkarni A M, Chatterjee A P, Schweizer K S and Zukoski C F 1999 *Phys. Rev. Lett.* **83** 4554
Farnum M and Zukoski C 1999 *Biophys. J.* **76** 2716
[9] Muschol M and Rosenberger F 1995 *J. Chem. Phys.* **103** 10424
[10] Muschol M and Rosenberger F 1997 *J. Chem. Phys.* **107** 1953
[11] Caccamo C 1996 *Phys. Rep.* **274** 1
[12] Hagen M H J and Frenkel D 1994 *J. Chem. Phys.* **101** 4093
[13] Piazza R, Peyre V and Degiorgio V 1998 *Phys. Rev.* E **58** R2733
[14] Vliegenthart G A, Lodge J M F and Lekkerkerker H N W 1999 *Physica* A **263** 378
[15] Israelachvili J N 1992 *Intermolecular and Surface Forces* 2nd edn (London: Academic)
[16] Nägele G 1996 *Phys. Rep.* **272** 215
[17] Beretta S, Chirico G and Baldini G 2000 *Macromolecules* **33** 8663
[18] Rosenberger F, Howard S B, Sowers J W and Nyce T A 1993 *J. Cryst. Growth* **129** 1
[19] Cacioppo E and Pusey M L 1991 *J. Cryst. Growth* **114** 286
Ewing F, Forsythe E and Pusey M L 1994 *Acta Crystallogr.* D **50** 424
[20] Panagiotopoulos A Z 1987 *Mol. Phys.* **61** 813
[21] Zerah G and Hansen J-P 1986 *J. Chem. Phys.* **84** 2336
[22] Caccamo C and Pellicane G 2002 *J. Chem. Phys.* **117** 5072
[23] Hansen J-P and McDonald I R 1986 *Theory of Simple Liquids* 2nd edn (London: Academic)
[24] Hall K R 1972 *J. Chem. Phys.* **57** 2252
Choi Y, Ree T and Ree H F 1991 *J. Chem. Phys.* **95** 7548
[25] Vliegenthart G A and Lekkerkerker H N W 2000 *J. Chem. Phys.* **112** 5364
[26] Noro M G and Frenkel D 2000 *J. Chem. Phys.* **113** 2941
[27] Haas C, Drenth J and Wilson W W 1999 *J. Phys. Chem.* B **103** 2808
[28] Asherie N, Lomakin A and Benedek G B 1996 *Phys. Rev. Lett.* **77** 4832
[29] Broide M, Tominc T M and Saxowsky M D 1996 *Phys. Rev.* E **53** 6325
[30] Taratuta V, Holschbach A, Thutston G M, Blankschtein D and Benedek G B 1990 *J. Phys. Chem.* **94** 2140
Petsev D N and Yekilov P G 2000 *Phys. Rev. Lett.* **84** 1339
[31] Neal B L, Asthagiri D, Velev O D, Lenhoff A M and Kaler E W 1999 *J. Cryst. Growth* **196** 377
[32] Piazza R 1999 *J. Cryst. Growth* **196** 415

[33] Boström M, Williams D R M and Ninham B W 2001 *Phys. Rev. Lett.* **87** 168103
[34] Dixit N M and Zukoski C F 2002 *J. Chem. Phys.* **117** 8540
[35] Sear R P 1999 *J. Chem. Phys.* **111** 4800
Warren P B 2002 *J. Phys.: Condens. Matter* **14** 7617
Lomakin A, Asherie N and Benedek G B 1999 *Proc. Natl Acad. Sci. USA* **96** 9465
[36] Allahyarov E, Löwen H, Louis A A and Hansen J-P 2002 *Europhys. Lett.* **57** 731
Allahyarov E, Löwen H, Louis A A and Hansen J-P 2002 *Preprint* http://www.arXiv.org/abs/cond-mat/0205551
[37] Costa D, Ballone P and Caccamo C 2002 *J. Chem. Phys.* **116** 3327
[38] Foffi G, McCullagh G D, Lawlor A, Zaccarelli E, Dawson K A, Sciortino F, Tartaglia P, Pini D and Stell G 2002 *Phys. Rev.* E **65** 031407 and references therein